

Effect of temperature on the photoluminescence of Eu^{3+} doped TiO_2 nanofibers prepared by electrospinning

J. ZHAO, H. DUAN, Z. MA, L. LIU, E. XIE*

Key Laboratory for Magnetism and Magnetic Materials of the Ministry of Education, Lanzhou University, Gansu, China 73000

Eu^{3+} doped titania ($\text{TiO}_2:\text{Eu}^{3+}$) nanofibers were synthesized by the electrospinning technique. The samples were calcined at different temperature in air. The structural and spectral information of the samples was characterized by field emission scanning electron microscopy (FESEM), x-ray diffraction (XRD), Raman spectrum, photoluminescence (PL). FESEM reveal that the nanofibers have the diameter between 30 and 70 nm. XRD measurements show that the crystal structure transforms from anatase to rutile phase with the increasing of calcined temperature. The photoluminescence spectra exhibit visible emission peaks centered at 550, 590, and 612, 660 nm due to $^5\text{D}_1-^7\text{F}_1$, $^5\text{D}_0-^7\text{F}_1$, $^5\text{D}_0-^7\text{F}_2$ and $^5\text{D}_0-^7\text{F}_3$ transition of Eu^{3+} ions and the PL intensities increase with the increasing of calcined temperature. At lower temperature this is attributed to the energy transfer from TiO_2 host to the Eu^{3+} ions. But at higher calcined temperature, near-infrared photoluminescence peaking at 815 nm appears due to the rutile TiO_2 and the intensity of visible photoluminescence decreases, which is attributed to pure phase TiO_2 host and the energy back transfer from Eu^{3+} ions to the TiO_2 host.

(Received August 15, 2008; accepted October 30, 2008)

Keywords: Nanofibers, Calcined temperature, Electrospinning, Photoluminescence

1. Introduction

In recent years, much attention has been paid to nanomaterials due to their unique optical and electric properties, which mainly come from high surface/volume ratio and the quantum size effect [1-3]. Rare earth element-doped semiconductors have been reported to be versatile light-emitting materials for wavelengths in the range from visible to near infrared. It has been reported that the luminescent quantum efficiency of Eu^{3+} in nanowires was enhanced more considerably than that of the corresponding nanoparticles and the bulk powders [4]. Eu^{3+} ions have been studied in different host materials, such as Gd_2O_3 , Y_2O_3 , TiO_2 , ZnO and Lu_2O_3 , GaN [5-10]. Titania (TiO_2) has been used as the favorable host material for rare earth elements, due to its outstanding optical and thermal properties and high chemical mechanical stability. Eu^{3+} ion is considered to be a good candidate for red luminescence centers of photoelectric devices due to its sharp and intense luminescence at room temperature.

Electrospinning is a simple and effective method for fabricating ultrafine nanofibers from a rich variety of functional materials that are exceptionally long in length and uniform in diameter [11]. The diameter of fibers prepared by this method can range from tens of nanometers to several micrometers. In a typical electrospinning setup, high voltage is applied to a droplet of polymer solution that rests on a sharp conducting dip. As a result of molecular ionization and charge redistribution, a Taylor cone is formed and a jet of the solution is extracted. The formed jet is then accelerated by the electric field and collector. When a volatile solvent is used, in-flight solvent evaporation occurs, hardening the fibers composed of the dissolved material, which are deposited on the substrate.

$\text{TiO}_2:\text{Eu}^{3+}$ thin films have been widely studied [12]. However, $\text{TiO}_2:\text{Eu}^{3+}$ nanofibers were rarely investigated. In this paper, we fabricate $\text{TiO}_2:\text{Eu}^{3+}$ nanofibers by electrospinning and studied the effect of calcined temperature on their photoluminescence properties.

2. Experiment details

In the first step, TiO_2 sol was prepared by dissolving 0.5 g Tetra-n-butyl titanate ($\text{Ti}(\text{OC}_4\text{H}_9)_4$) (>98%) into 1 ml ethanol and 1 ml acetic acid was used as a catalyst. Then europium nitrate was added into the obtained TiO_2 sol, the concentration of the doped Eu^{3+} ions is controlled to be 3 mol%. The obtained sol was placed for about 20 minutes to allow the Tetra-n-butyl titanate hydrolyzing. Second this solution was added to 2 ml of ethanol that contained 0.2 g Polyvinylpyrrolidone (PVP) (Sigma-Aldrich, $M_w \approx 1\,300\,000$) and 0.5 ml of N, N - dimethyl formamide (DMF), followed by magnetic stirring for ~1h. Then the obtained mixed solution was loaded into a syringe equipped with a stainless needle with the diameter of 0.6 mm. Silicon plates were placed on the zinc flake to collect the electrospun nanofibers. The distance between the tip of the needle and zinc flake is 15 cm. Upon applying a high voltage of 25 kV, a fluid jet was ejected from the needle tip. The solvent evaporated and a charged nanofibers was deposited on the collector. The as-spun composite nanofibers on silicon wafers were left in air for ~24 h to allow $\text{Ti}(\text{OC}_4\text{H}_9)_4$ hydrolyzed completely. The collected nanofibers were calcined at 400°C, 600°C, and 800°C for 3 h in air.

The samples were characterized by field emission scanning electron microscopy (FESEM) (Hitachi, S-4800), X-ray diffraction (XRD) (Philips, Regiku D/max-IIIc (Cu

Ka ray)), Raman (JY-HR800, 532 nm). Room temperature PL emission spectra of $\text{TiO}_2:\text{Eu}^{3+}$ nanofibers were recorded using a 325 nm He-Cd laser as an excitation source (RF-540).

3. Results and discussion

FESEM images of $\text{TiO}_2:\text{Eu}^{3+}$ nanofibers calcined at 400°C, 600°C, and 800°C in air for 3 h are shown in Fig. 1(a-c), respectively. It can be seen from Figure 1 (a and b) that the nanofibers calcined at 400°C and 600°C have a relatively smooth surface and align in random orientation because of the bending instability associated with the spinning jet. The nanofibers are relatively straight and the diameter of nanofibers is between 30 nm and 100 nm while the diameter hardly varies with calcination temperature. There is only a little PVP and organic compounds after calcined at 400°C for 3 h, so the diameters of nanofiber hardly vary with the increasing of calcination temperature. The $\text{TiO}_2:\text{Eu}^{3+}$ nanofibers obtained after calcined at 800°C for 3 h shows a different morphology (Fig. 1(c)). It is noticeable that the nanofibers show burl-like wavy surfaces and consist of linked crystalline particles or crystallites. This morphology seems to be related to a dramatic change in crystalline structure.

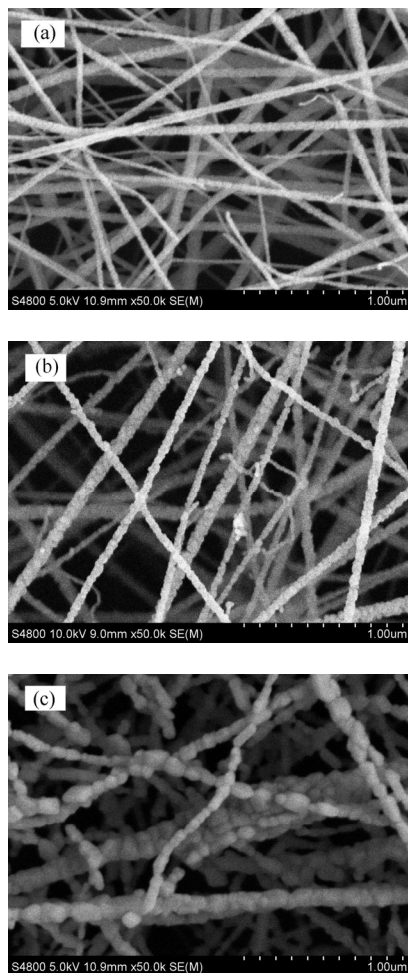


Fig. 1. FESEM images of $\text{TiO}_2:\text{Eu}^{3+}$ nanofibers calcined at 400°C, 600°C, and 800°C in air for 3 h, respectively.

Fig. 2 shows XRD patterns of the $\text{TiO}_2:\text{Eu}^{3+}$ (Eu^{3+} concentration 3%) nanofibers samples at calcined at (A) 400°C, (B) 600°C, (C) 800°C. For $\text{TiO}_2:\text{Eu}^{3+}$ nanofibers annealed at 400°C and 600°C ((A) and (B)), the XRD peaks at $2\theta = 25.2, 37.5, 48$ and 55.1 can be assigned to the diffraction of (101), (004), (200), and (105) plains of anatase TiO_2 . No diffraction peak of organic compounds can be observed, implying that most of the PVP has been evaporated at this calcination temperature. The sample calcined at 800°C for 3 h shows mixed crystalline phases of anatase and rutile, as shown Figure 2(C). The peaks at $2\theta = 27.3, 36.1, 41.2$ and 54.4 can be assigned to the diffraction of (110), (101), (111), and (211) plains of rutile TiO_2 and the peak at $2\theta = 25.2$ is assigned to anatase TiO_2 .

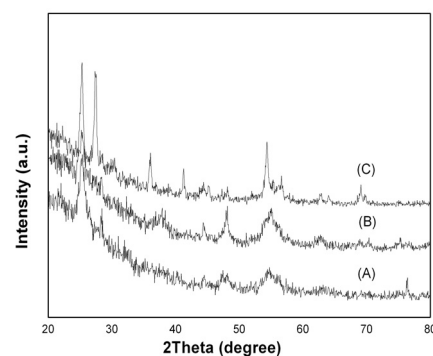


Fig. 2. XRD patterns of $\text{TiO}_2:\text{Eu}^{3+}$ nanofibers calcined at (A) 400°C, (B) 600°C, (C) 800°C for 3h, respectively.

The ratio between anatase and rutile extracted from XRD spectra was computed with the empirical relationship used by Depero *et al* [13].

$$R(T) = 0.679 \frac{I_R}{I_R + I_A} + 0.312 \left(\frac{I_R}{I_R + I_A} \right)^2$$

where $R(T)$ is the percentage content of rutile at each temperature, I_A is the intensity of the main anatase reflection (101) ($2\theta = 25.2^\circ$), and I_R is the intensity of the main rutile reflection (110) ($2\theta = 27.3^\circ$). The result of the sample calcined at 800°C for 3 h is 82%, so the main phase is ascribed to rutile TiO_2 . No peaks from the europium compound and no shift of the anatase and rutile peaks are detected after doping Eu^{3+} , indicating that the incorporation of Eu^{3+} ions does not change the structure of the TiO_2 nanofibers. With the doping of Eu^{3+} in the samples, the phase transition temperature is elevated [14]. This indicates that the annealing temperature required for the anatase-to-rutile phase transformation of TiO_2 nanofibers is increased due to the doping of Eu^{3+} ions.

Raman spectra measurements were carried out on nanofibers calcined at temperature ranging from 400°C to 800°C (Figure 3(a), (b) and (c)). For Figure 3(a) and (c),

the Raman lines at 146, 399, and 639 cm^{-1} are assigned to the Eg, B1g, and Eg modes of the TiO_2 anatase phase, respectively. The intensity of the whole peaks increases with the increasing of calcination temperature, this indicates that the crystalline of sample elevates with the increasing of calcination temperature. But the sample obtained after calcination up to 800°C (Fig. 3(c)) is identified as a mixture of rutile, as the dominant phase, and anatase. The main Raman lines at 450 and 612 cm^{-1} are assigned to the Eg and A1g modes of the TiO_2 rutile phase, respectively. The Raman line at 146 cm^{-1} is ascribed to the anatase phase. These results of phase transition are well in agreement with the results measured by XRD.

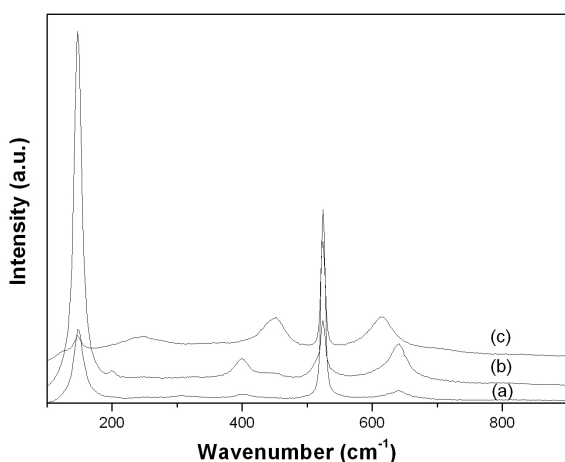


Fig. 3. Raman spectra of $\text{TiO}_2:\text{Eu}^{3+}$ nanofibers calcined in air at (a) 400°C , (b) 600°C , (c) 800°C for 3h, respectively.

Figure 4 shows the calcination temperature effect of $\text{TiO}_2:\text{Eu}^{3+}$ nanofibers on the luminescence spectra. The samples were excited by the He-Cd laser at wavelength of 325 nm. The calcination temperature plays an important role in the photoluminescence intensity of $\text{TiO}_2:\text{Eu}^{3+}$ nanofibers. The intensity of the main emission peak at 612 nm increases with the increasing of calcination temperature from 400°C to 600°C , meanwhile other weaker emissions at 550, 590, and 660 nm are detected, which are assigned to intra-4f transition of ${}^5\text{D}_1-{}^7\text{F}_1$, ${}^5\text{D}_0-{}^7\text{F}_1$, and ${}^5\text{D}_0-{}^7\text{F}_3$, respectively. The peak at 612 nm is caused by the electron dipole transition of Eu^{3+} (${}^5\text{D}_0-{}^7\text{F}_2$), induced by the lack of inversion symmetry at the Eu^{3+} site, the ${}^5\text{D}_0-{}^7\text{F}_2$ transition is highly sensitive to the environment around Eu^{3+} , hence, the calcination temperature is strongly influence its strength. The emission near 590 nm is due to the magnetic dipole transition, which is insensitive to the environment around the Eu^{3+} ions. After the calcination temperature up to 800°C , the intensity of red emission peaks decreases and the near-infrared emission peaking at about 820 nm appears. Photoluminescence transitions associated Ti^{3+} interstitial ions in rutile single crystal have

been reported, with the emission peak at 820 nm [15] In the basic TiO_2 cell, each Ti^{4+} is surrounded by an octahedron of six O^{2-} ions, a structural defect can be formed by losing a neutral oxygen atom during high temperature annealing and the defect states associated with Ti^{3+} ions are introduced in the band gap at 0.7-0.8 eV below E_F [16]. We conclude that the 820 nm PL of $\text{TiO}_2:\text{Eu}^{3+}$ is attributed to TiO_2 host.

From XRD and Raman spectra, we can see that the $\text{TiO}_2:\text{Eu}^{3+}$ nanofibers after calcination at 600°C and 800°C have different crystalline phase. The nanofibers calcined 800°C is the mixture of anatase and rutile phase. It has been reported that the structural differences for the anatase and rutile govern the differences of their electrical and optical properties [17-18]. For the anatase nanofibers, the electrons are excited to the conduction band of TiO_2 nanofibers by absorbing the photon energy for the 325 nm wavelength, and this energy is directly transferred to Eu^{3+} ions from TiO_2 nanofibers. For rutile TiO_2 nanofibers, the energy of 1.53 eV associated with Ti^{3+} interstitial ions is lower than that transition energy of Eu^{3+} ions associated with intra-4f transition ${}^5\text{D}_1-{}^7\text{F}_1$, ${}^5\text{D}_0-{}^7\text{F}_j$ ($j=1,2,3$). The energy will be to back transferred from Eu^{3+} to defect level associated with Ti^{3+} interstitial ions. Furthermore 820 nm emission of $\text{TiO}_2:\text{Eu}^{3+}$ is stronger than that of pure TiO_2 nanofibers in other article [19]. So we can conclude the energy back transfer is responsible for the luminescence of 820 nm.

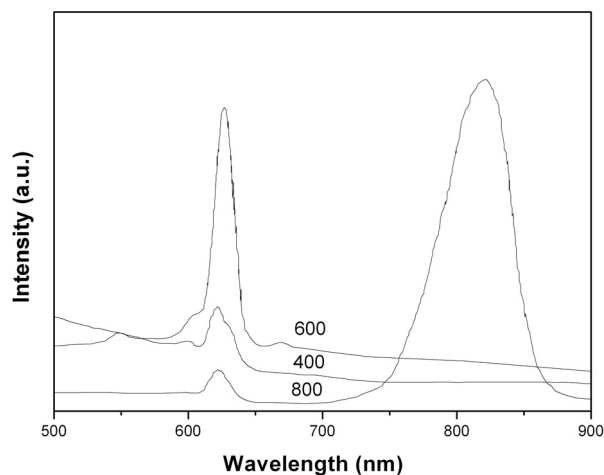


Fig. 4. PL spectra of $\text{TiO}_2:\text{Eu}^{3+}$ nanofibers calcined in air at 400, 600 and 800°C for 3h, respectively.

4. Conclusions

$\text{TiO}_2:\text{Eu}^{3+}$ nanosized fibers have been successfully prepared using electrospinning method. The samples were calcined at various temperature in air for 3h. Eu^{3+} -doped nanofibers restrain the phase transition temperature of TiO_2 in comparison to undoped nanofibers. With the increase of calcining temperature, PL intensity due to the

Eu³⁺ ions increases firstly but then decreases and PL intensity due to rutile phase TiO₂ appears and is stronger than undoped nanofibers. It can be explained that the energy back transfer from Eu³⁺ to defect states associated with Ti³⁺ interstitial ions of rutile phase dominates the emissions at high calcining temperatures.

Acknowledgment

We thank the Program for New Century Excellent Talents in the University in China for the financial support.

References

- [1] L. Q. Liu, E. Ma, R. F. Li, G. K. Liu, X. Y. Chen, *Nanotechnology* **18** 015403 (2007).
- [2] P. D. Yang, H. Q. Yan, S. Mao, R. Russo, J. Johnson, R. Saykally, N. Morris, J. Pham, R. R. He, H. J. Choi, *Adv. Funct. Mater.* **12** 323 (2000).
- [3] A. V. Murugan, O. Y. Heng, V. Ravi, A. K. Viswanath, K. Vijayamohanan, *J. Mater. Sci.* **41** 1459 (2006).
- [4] H. Song, L. Yu, S. Lu, T. Wang, Z. Liu, L. Yang, *Appl. Phys. Lett.* **85**, 840 (2004).
- [5] L. Q. Liu, X. Y. Chen, *Nanotechnology* **18** 255704 (2007).
- [6] Z. L. Fu, S. H. Zhou, T. Q. Pan, S. Y. Zhang, *J. Lumin.* **124** 213 (2007).
- [7] Q. G. Zeng, Z. M. Zhang, Z. J. Ding, Y. Wang, Y. Q. Sheng, *Scripta Mater.* **57**, 897 (2007).
- [8] M. Y. Zhong, G. Y. Shan, Y. J. Li, G. R. Wang, Y. C. Liu, *Mater. Chem. and Phys.* **106** 305 (2007).
- [9] X. J. Liu, H. L. Li, R. J. Xie, N. Hirosaki, X. Xu, L. P. Huang, *J. Lumin.* **127** 469 (2007).
- [10] C. K. Xu, J. W. Chun, B. W. Chon, T. H. Joo, D. E. Kim, *Nanotechnology* **18** 015703 (2007).
- [11] D. Li, Y. N. Xia, *Adv. Mater.* **14** 1151 (2004).
- [12] A. C. Gallardo, M. G. Rocha, I. H. Calderon, R. P. Merino, *Appl. Phys. Lett.* **78** 3436 (2001).
- [13] L. E. Depero, L. Sangaletti, B. Allieri, E. Bontempi, R. Salari, M. Zocchi, C. Casale, M. Notaro, *J. Mater. Res.* **13** 1644 (1998).
- [14] Q. G. Zeng, Z. J. Ding, Z. M. Zhang, *J. Lumin.* **118** 301 (2006).
- [15] A. K. Ghosh, F. G. Wakim, R. R. Addiss Jr, *Phys. Rev.* **184** 979 (1969).
- [16] H. Tang, K. Prasad, R. Sanjines, P. E. Schmid, F. Levy, *J. Appl. Phys.* **75**, 2945 (1994).
- [17] S. D. Mo, W. Y. Ching, *Phys. Rev. B* **51**, 13023 (1995).
- [18] U. Diebold, *Surf. Sci. Rep.* **48**, 53 (2003).
- [19] Jianguo Zhao, Changwen Jia, Huigao Duan, Hui Li, Erqing Xie, *J. Alloy Compd.* **455**, 497 (2008).

*Corresponding author. xieeq@lzu.edu.cn